Stability of the Dimerization Domain Effects the Cooperative DNA Binding of Short Peptides†

Yasunori Aizawa,‡ Yukio Sugiura,‡ Masaru Ueno,§ Yasuo Mori,|| Keiji Imoto,|| Keisuke Makino,⊥ and Takashi Morii*,⊥

Institute of Advanced Energy, Kyoto University, Uji, Kyoto 611-0011, Institute for Chemical Research, Kyoto University, Uji, Kyoto 611-0011, Department of Chemistry, Shizuoka University, Oya, Shizuoka 422, and Department of Information Physiology, National Institute for Physiological Sciences, Okazaki, Aichi 444, Japan

Received December 7, 1998; Revised Manuscript Received January 26, 1999

ABSTRACT: The basic region peptide derived from the basic leucine zipper protein GCN4 bound specifically to the native GCN4 binding sequences in a dimeric form when the β-cyclodextrin/adamantane dimerization domain was introduced at the C-terminus of the GCN4 basic region peptide. We describe here how the structure and stability of the dimerization domain affect the cooperative formation of the peptide dimer−DNA complex. The basic region peptides with five different guest molecules were synthesized, and their equilibrium dissociation constants with a peptide possessing β-cyclodextrin were determined. These values, ranging from 1.3 to 15 μM, were used to estimate the stability of the complexes between the dimers with various guest/cyclodextrin dimerization domains and GCN4 target sequences. An efficient cooperative formation of the dimer complexes at the GCN4 binding sequence was observed when the adamantyl group was replaced with the norbornyl or noradamantyl group, but not with the cyclohexyl group that formed a β-cyclodextrin complex with a stability that was 1 order of magnitude lower than that of the adamantyl group. Thus, cooperative formation of the stable dimer−DNA complex appeared to be effected by the stability of the dimerization domain. For the peptides that cooperatively formed dimer−DNA complexes, there was no linear correlation between the stability of the inclusion complex and that of the dimer−DNA complex. With the β-cyclodextrin/adamantane dimerization domain, the basic region peptide dimer preferred to bind to a palindromic 5′-ATGACGTCAT-3′ sequence over the sequence lacking the central G·C base pair and that with an additional G·C base pair in the middle. Changing the adamantyl group into a norbornyl group did not alter the preferential binding of the peptide dimers to the palindromic sequence, but slightly affected the selectivity of the dimer for other nonpalindromic sequences. The helical contents of the peptides in the DNA-bound dimer with the adamantyl group were decreased by reducing the stability of the dimer−DNA complex, which was possibly caused by deformation of the helical structure proximal to the dimerization domain.

Sequence-specific DNA binding proteins often play crucial roles in the dimeric form when targeting specific DNA sequences of the gene regulatory elements (*1*, and references cited therein, *2*). X-ray crystallographic studies of many protein−DNA complexes have provided useful information about the hydrogen-bonded interactions and hydrophobic contacts between amino acid residues in the protein and the functional group in DNA (*3*, *4*). In addition to these direct contacts, noncovalent and specific protein−protein interactions between the protein monomers are also important for the highly specific molecular recognition mechanisms associated with protein−DNA interactions (*5*−*7*). However, structural elements of natural proteins are less easily separated for studying the role of dimer formation in modulating the affinity and cooperativity of protein−DNA interactions (*6*−*10*).

A host−guest inclusion complex of β-cyclodextrin (Cd) and adamantane (Ad) provides a new method for associating oligopeptides in an aqueous solution (*11*−*13*). By using this method, it is possible to design DNA binding peptides capable of forming functional homo- (*11*) and heterodimers (*12*) and homo-oligomers (*13*) of short peptides through noncovalent interactions. The basic region peptide derived from the basic leucine zipper (bZIP) protein GCN4 (*14*−*16*) binds specifically to the native GCN4 binding sequences in a dimeric form when the noncovalent Ad/Cd dimerization domain is introduced at the C-terminus of the basic region peptide (*11*). Although a number of studies on the DNA binding of the basic region peptide dimers have been reported, most of these peptide dimers are formed with covalent linkages, such as a disulfide bond (*17*−*20*), a transition metal complex (*21*−*23*), chiral bridged biphenyl derivatives (*24*−*26*), and a lysine residue (*27*). Our system provides a unique opportunity to study roles of the nonco-

† This work was supported by a Grant-in-Aid for Scientific Research (09680569) from the Ministry of Education, Science, Sports and Culture, Japan, to T.M. and "Research for the Future" Program Grant JSPS-RFTF 96L00207 from the Japan Society for the Promotion of Science to K.I. Y.A. is a research fellow of the Japan Society for the Promotion of Science.

* To whom correspondence should be addressed: Institute of Advanced Energy, Kyoto University, Uji, Kyoto 611-0011, Japan. Telephone: +81-774-38-3585. Fax: +81-774-38-3524. E-mail: t-morii@iae.kyoto-u.ac.jp.

‡ Institute for Chemical Research, Kyoto University.

§ Shizuoka University.

|| National Institute for Physiological Sciences.

⊥ Institute of Advanced Energy, Kyoto University.

10.1021/bi9828829 CCC: $18.00
Published on Web 03/12/1999

valent interaction between the peptides in the DNA binding of peptide dimers.

In the case of native protein dimers, reducing the dimerization ability by using the deletion mutants may complicate the situation (*8*−*10*). It is difficult to measure the dimerization ability directly, and these mutations may give an undesired effect on the folding of the DNA binding domain. In contrast, the β-Cd/Ad dimerization domain is modular and gives rise to little conformational change in the process of inclusion complex formation. In addition, β-Cd forms specific 1:1 complexes with many guest molecules in an aqueous solution (*30*, *31*). We postulated that the stability of the β-Cd/guest dimerization domain can be independently controlled by changing the guest molecules without greatly affecting the DNA binding ability of the peptide itself. We have used the basic region peptide derived from the bZIP protein to test the validity of the β-Cd/guest dimerization domain. The GCN4 basic region peptide was chosen as a DNA binding domain because the basic region peptide of the bZIP protein alone was sufficient for the sequence-specific DNA binding upon dimerization (*17*, *18*, *21*−*26*). In this study, we have prepared a series of guest peptides that differed only in the guest molecule to explore roles of the noncovalent dimerization domain in the cooperative formation of peptide dimer−DNA complexes. The results indicate that the stability of the inclusion complex dominantly controls the cooperative formation of the dimer−DNA complex, and that the shape and size of the dimerization domain significantly affect the sequence selectivity of peptide dimers.

MATERIALS AND METHODS

Materials. Protected Fmoc (9-fluorenylmethoxycarbonyl) amino acids and PyBOP [bromo-tris(pyrrolidino)phosphonium hexafluorophosphate] were obtained from Novabiochem. 1-Hydroxybenztriazole (HOBt) was from Nakaraitesque. Fmoc-PAL-PEG resin (0.2 mmol/g) was from PerSeptive Biosystems. Dimethylformamide was dried over CaH_2, distilled from ninhydrine at 55 °C under reduced pressure, and stored over 4 Å molecular sieves. Protected nucleoside phosphoramidites were obtained from PerSeptive. *N*-Hydroxysuccinimidyl-6-(biotinamido) hexanoate was purchased from Vector Laboratories, Inc. T4 polynucleotide kinase was obtained from New England Biolabs. [γ-^{32}P]-Adenosine 5′-triphosphate (>6000 Ci/mmol) was from Amersham. HPLC grade acetonitrile was employed for both analytical and preparative HPLC. A reagent grade Milli-Q water was used throughout the experiments. All other chemicals were reagent grade and were used without further purification. Sensor chip SA and Sephadex G-10 and G-25 were obtained from Pharmacia. A reverse-phase C18 column (20 mm × 250 mm, Ultron VX-Peptide, Sinwa Chemical Industry) was used for purification of peptides for preparative purposes. Analytical HPLC was carried out on a reverse-phase C18 column (4.6 mm × 150 mm, Ultron VX-Peptide, Sinwa Chemical Industry). Oligonucleotides were purified on a reverse-phase C18 column (6 mm × 150 mm, Ultron VX-Nucleotide, Sinwa Chemical Industry). Amino acid analyses were performed with an AccQ Tag Chemistry Package (Waters) according to company protocol. Surface plasmon resonance spectra were obtained on a Pharmacia BIAcore2000 biosensor. Electrospray mass spectrometry was carried out in the positive ion mode on a Perkin-Elmer Sciex API III instrument.

Synthesis of G23Ad, G23NAd, G23Nb, G23NrA, and G23Ch. G23Ad was synthesized by reaction of G23 (*11*) (10 mg, 3.6 mmol) with *N*-(bromoacetyl)-1-adamantanemethylamine (17 mg, 60 mmol) in aqueous DMF solution (pH 9, 3:2 water/DMF) at 0 °C under nitrogen. After 1 h, the reaction was quenched by addition of acetic acid, and the mixture was passed through a Sephadex G-10 column. Successive purification with a reversed-phase HPLC system gave pure G23Ad (8 mg, 74% yield). The HPLC conditions were as follows: eluent A, 0.1% TFA/water; eluent B, 0.1% TFA/water containing 50% CH_3CN; and flow rate, 6 mL/min. MS (electrospray, 50% acetonitrile, 0.05% formic acid) calcd for [M^+] 2983.7, found 2985.8. G23NAd, G23NrA, G23Nb, and G23Ch were synthesized in a similar manner from G23 with *N*-(bromoacetyl)aminoadamantane, *N*-(bromoacetyl)aminonoradamantane, *N*-(bromoacetyl)-2-aminoethylnorbornane, and *N*-(bromoacetyl)cyclohexylamine, respectively. MS for G23NAd (electrospray, 50% acetonitrile, 0.05% formic acid) calcd for [M^+] 2969.7, found 2969.9. MS for G23NrA (electrospray, 50% acetonitrile, 0.05% formic acid) calcd for [M^+] 2955.7, found 2955.2. MS for G23Nb (electrospray, 50% acetonitrile, 0.05% formic acid) calcd for [M^+] 3044.7, found 3043.7. MS for G23Ch (electrospray, 50% acetonitrile, 0.05% formic acid) calcd for [M^+] 3141.8, found 3141.1. Structures and amino acid sequences of G23Ad, G23NAd, G23Nb, G23NrA, and G23Ch are shown in Figure 1B. A stock solution containing each G23-guest peptide was prepared by dissolving the peptide in TE buffer [1 mM Tris-HCl and 0.1 mM EDTA (pH 8.0)]. Peptide concentrations were determined by quantitative amino acid analyses.

Synthesis of G23Cd. G23Cd was synthesized by a reaction of G23 (13 mg, 4.6 mmol) with mono-6-deoxy-6-iodo-β-cyclodextrin (*32*) (124 mg, 100 mmol) in 100 mM phosphate buffer (pH 9) at 0 °C under nitrogen for 5 h. The reaction was quenched by an addition of acetic acid, and the mixture was passed through a Sephadex G-10 column. G23Cd was purified with a reverse-phase HPLC system. HPLC conditions were as follows: eluent A, 0.05% TFA/water; eluent B, 0.05% TFA/water containing 50% CH_3CN; and flow rate, 5 mL/min. After HPLC purification, the mobile-phase solution containing G23Cd was neutralized by an addition of triethylamine, and resulting triethylammonium trifluoroacetate was removed by passing the mixture through a Sep-pak C18 cartridge. Lyophilization of this desalted solution yielded pure G23Cd (5.5 mg, 38% yield). MS (electrospray, 50% acetonitrile, 0.05% formic acid) calcd for [M^+] 3899.8, found 3895.0. A stock solution containing G23Cd was prepared by dissolving the peptide in TE buffer [1 mM Tris-HCl and 0.1 mM EDTA (pH 8.0)]. BG23Cd was synthesized by a reaction of bioG23 (13 mg, 4.6 mmol), which was synthesized in a similar manner as described previously for G23 (*11*) except the final capping reaction with a 2-fold molar excess of *N*-hydroxysuccinimidyl-6-(biotinamido) hexanoate, with mono-6-deoxy-6-iodo-β-cyclodextrin as described above. The peptide concentration was determined by a quantitative amino acid analysis.

Synthesis and 5′-End Labeling of Oligonucleotides AP20, CRE21, CGG22, and NON. Oligonucleotides were synthesized on a PerSeptive DNA synthesizer with the standard phosphoramidite method and purified by reverse-phase

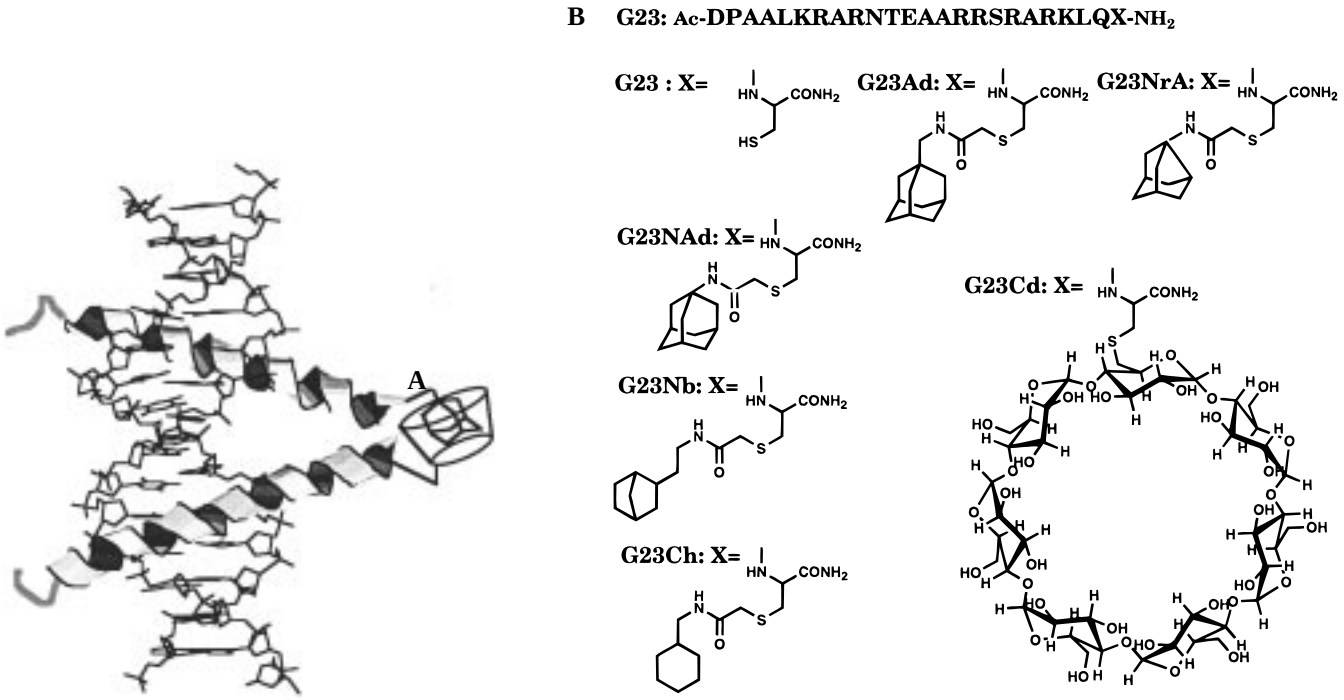

FIGURE 1: (A) Schematic representations showing the G23Ad/G23Cd dimer bound at the AP1 sequence. Gray ribbons represent the basic region peptides in the helical conformation. Shown at the C-terminus of the helices are β-cyclodextrin and the adamantyl group. Coordinates for the basic region peptides and DNA were adopted from the GCN4−AP1 complex (*28*), and the ribbon representation was generated by the program MolView (version 1.3) (*29*). (B) Amino acid sequence for the G23 peptide and structures of the modified C-terminal Cys residue (X). The cysteine residues were modified with 6-deoxy-6-iodo-β-cyclodextrin for G23Cd and with bromoacetyl derivatives of the guest molecules for G23Ad, G23NAd, G23NrA, G23Nb, and G23Ch.

HPLC on an Ultron VX-Nucleotide column (Sinwa Chemical Industry, 6 mm × 150 mm) with 0.1 M triethylammonium acetate/acetonitrile as an eluent. The oligonucleotides were labeled by kinase reaction using [γ-^{32}P]ATP (>6000 Ci/mmol) and T4 polynucleotide kinase (*33*), followed by removal of unincorporated label over Sep-pak. The oligonucleotide was then denatured and annealed to a 4-fold molar excess of the opposite strand in 25 mM Tris-HCl, 100 mM NaCl, and 1 mM EDTA at pH 8.0. Nucleotide sequences of the oligonucleotides used in this study are 5′-CGGATGACTCATTTTTTTTC-3′ (AP20), 5′-CGGATGACGTCATTTTTTTTC-3′ (CRE21), 5′-CGGATGACGGTCATTTTTTTTC-3′ (CGG22), and 5′-GATCCCCCCAACACCTGCTGCCTGA-3′ (NON).

Electrophoretic Mobility Shift Assay. Typical binding reactions were carried out in the presence of the indicated peptide with ~20 pM 5′-^{32}P-labeled oligonucleotide (double-stranded) in a binding mixture containing 20 mM Tris-HCl (pH 7.5), 4 mM KCl, 2 mM $MgCl_2$, 1 mM EDTA, and 6% sucrose. The binding mixtures were incubated at the indicated temperature for 30 min, and an aliquot (8 μL) of each binding mixture was directly loaded onto an 8% nondenaturing acrylamide gel (29:1 acrylamide/bis-acrylamide), carried out in TBE buffer (20 mM Tris, 20 mM boric acid, and 0.1 mM EDTA) at the indicated temperature, and analyzed by autoradiography (*34*, *35*). Gel electrophoresis was performed in ATTO AE-6410 gel boxes cooled by a temperature-regulated circulating methanol/water bath. The temperature of the buffer was maintained at the indicated temperature, and the gels were thermally equilibrated and pre-electrophoresed for 45 min in an apparatus prior to loading the samples. The increase in the mobility-shifted band was quantitated by the densitometry of the autoradiogram. The concentration of the peptide was determined by quantitative amino acid analysis with α-aminobutyric acid as an internal standard.

Determination of Equilibrium Dissociation Constants for the G23-Guest/G23Cd Complexes. The principle of operation of the BIAcore biosensor has been described previously (*36*). N-Terminal biotinylated peptide (BG23Cd) was injected over a streptavidin-coated sensor chip (SA, Pharmacia Biosensor) until a suitable level (~800 RU) was achieved. Tris buffer (20 mM Tris-HCl and 150 mM KCl) was used as both a flow buffer and a sample preparation buffer. The same buffer containing 1 mM β-cyclodextrin was used as a regeneration buffer. G23 peptides with various guest molecules at their C-termini were analyzed typically at six different concentrations (1, 2, 5, 10, 20, and 50 μM). The association was followed for 12 min and the dissociation for 18 min at a flow rate of 30 μL/min.

Analysis of the data was performed using the evaluation software supplied with the instrument (BIAevaluation version 3.0). To eliminate small bulk refractive change differences at the beginning and end of each injection, a control sensorgram obtained over a surface modified with biotin was subtracted for each peptide injection. For the determination of the equilibrium dissociation constant (K_{d1}) from binding experiments

$$R = (R_{max}C)/(K_{d1} + C) \quad (1)$$

was used. R, R_{max}, and C are the response at equilibrium, the maximum response level, and the concentration of peptide, respectively. A range of peptide concentrations was injected, and the response at equilibrium was plotted against the peptide concentration. The data were analyzed using eq

1 to obtain estimates of the equilibrium dissociation constant, K_{d1}.

Analysis of Energetics by Electrophoretic Mobility Shift Titrations. All binding reactions were performed as described above at the indicated temperature, salt concentrations, and peptide concentrations. The equilibria and mass action involved in the overall DNA binding reaction of G23-guest and G23Cd peptides are

$$CG \overset{K_{d1}}{\rightleftharpoons} C + G \tag{2}$$

$$CGD \overset{K_{d2}}{\rightleftharpoons} CG + D \tag{3}$$

$$[G]_t = [G] + [CG] + [CGD] \tag{4}$$

$$[C]_t = [C] + [CG] + [CGD] \tag{5}$$

$$[D]_t = [D] + [CGD] \tag{6}$$

$$K_{d1} = [G][C]/[CG] \tag{7}$$

$$K_{d2} = [CG][D]/[CGD] \tag{8}$$

[G], [C], and [D] are, respectively, the free concentrations of G23-guest, G23Cd, and DNA. [CGD] represents a concentration of the G23-guest/G23Cd−DNA complex. $[C]_t$, $[G]_t$, and $[D]_t$ represent total concentrations of G23Cd, G23-guest, and DNA, respectively. K_{d1} and K_{d2} represent dissociation constants of the G23-guest/G23Cd−DNA complex and G23-guest/G23Cd dimer, respectively. Combining eqs 7 and 8 yields

$$K_{d1}K_{d2} = [G][C][D]/[CGD] \tag{9}$$

Substituting eq 6 into eq 9 leads to

$$[CGD] = [G][C][D]_t/(K_{d1}K_{d2} + [G][C]) \tag{10}$$

Combining eqs 4 and 5 yields

$$2[CG] = [G]_t + [C]_t - [G] - [C] - 2[CGD] \tag{11}$$

Under conditions where $[C]_t \gg [CGD]$ and $[G]_t \gg [CGD]$, $[C]_t - [CGD] \approx [C]_t$, and $[G]_t - [CGD] \approx [G]_t$, then eq 11 may be reduced to

$$2[CG] = [G]_t + [C]_t - [G] - [C] \tag{12}$$

Substituting eq 7 into eq 12 leads to

$$2[G][C]/K_{d1} = [G]_t + [C]_t - [G] - [C] \tag{13}$$

Because $[G]_t = [C]_t$ and $[G] = [C]$ in this work, eq 13 yields expression 14:

$$[G]^2 + K_{d1}[G] - K_{d1}[G]_t = 0 \tag{14}$$

Equation 14 is converted using the quadratic formula into expression 15

$$[G] = [-K_{d1} + (K_{d1}{}^2 + 4K_{d1}[G]_t)^{1/2}]/2 \tag{15}$$

The fraction of bound DNA (θ) can be expressed as

$$\theta = [CGD]/[D]_t \tag{16}$$

Substituting eqs 10 and 15 into eq 16 and setting [G] equal to [C] leads to

$$\begin{aligned}\theta &= [C][G]/(K_{d1}K_{d2} + [C][G]) \\ &= [G]^2/(K_{d1}K_{d2} + [G]^2) \\ &= 1/\{1 + 2K_{d2}/[K_{d1} + 2[G]_t - (K_{d1}{}^2 + 4K_{d1}[G]_t)^{1/2}]\}\end{aligned} \tag{17}$$

The K_{d2} was obtained by fitting the experimentally obtained binding data θ to the theoretical eq 17 with a nonlinear least-squares fitting program (IgorPro 2.02, WaveMetrics Inc., Lake Oswego, OR). The value for K_{d1} for each G23-guest peptide was taken from Table 1 and used as a fixed parameter.

Measurement of CD Spectra. Spectra of the peptide in the presence of oligonucleotides were calculated as the difference between the bound spectrum and a spectrum of the respective free oligonucleotide. CD spectra were obtained with a Jasco J-720 CD spectrometer equipped with a temperature controller set at 4 °C in a 1 mm cell. Samples contained 20 mM Tris-HCl (pH 7.5), 4 mM KCl, 2 mM $MgCl_2$, 1 mM EDTA, 4 μM peptide, and 5 μM oligonucleotide duplex when present. Spectra were the average of 32 scans and were corrected with a spectrum of buffer alone but not smoothed.

RESULTS

Stability of Inclusion Complexes between the Peptide with Cd and Peptides with Various Guest Molecules. A 23-residue peptide (G23) derived from the DNA contacting region of the transcriptional activator protein GCN4 (*14*−*16*) was synthesized by using a solid-phase method (*37*). N- and C-termini of G23 were acetylated and amidated, respectively, to avoid introducing additional charge interactions. Reaction of the C-terminal cysteine residue of G23 with *N*-(bromoacetyl)-1-adamantanemethylamine at 0 °C for 1 h gave G23Ad (Figure 1) quantitatively. G23NAd, G23NrA, G23Nb, and G23Ch were synthesized from G23 in a similar manner with *N*-(bromoacetyl)-1-aminoadamantane, *N*-(bromoacetyl)-1-aminonoradamantane, *N*-(bromoacetyl)-2-aminoethylnorbornane, and *N*-(bromoacetyl)-cyclohexylamine, respectively. G23Cd was synthesized by using mono-6-deoxy-6-iodo-β-cyclodextrin (*32*) (Figure 1).

Although equilibrium association constants for the complexes between β-Cd and guest molecules have been identified for many cases (*30*, *31*), the basic region peptides could affect the affinities between the G23Cd and G23-guest peptides. Equilibrium dissociation constants for the complexes of G23Cd and G23-guest peptides were determined by using the surface plasmon resonance technique (*36*). To immobilize the G23Cd peptide on a streptavidin-coated surface, G23 peptide containing a biotin group at the N-terminus (BG23) was prepared by capping the G23 peptide with *N*-hydroxysuccinimidyl-6-(biotinamido) hexanoate at the end of solid-phase peptide synthesis. The biotinyl peptide was modified with mono-6-deoxy-6-iodo-β-cyclodextrin to afford BG23Cd, which was then immobilized on a streptavidin-coated surface of the sensor chip.

Table 1: Equilibrium Dissociation Constants K_{d1} (Dimerization) and K_{d2} for the G23Ad/G23Cd, G23NAd/G23Cd, G23Nb/G23Cd, G23NrA/G23Cd, and G23Ch/G23Cd Complexes with AP20

guest peptide	K_{d1} (M)[a]	K_{d2} (M)[b]	ΔG (kcal/mol)[c]
G23Ad	$(1.34 \pm 0.25) \times 10^{-6}$	$(2.32 \pm 0.06) \times 10^{-11}$	−20.9
G23NAd	$(1.32 \pm 0.19) \times 10^{-6}$	$(1.22 \pm 0.06) \times 10^{-11}$	−21.3
G23Nb	$(3.09 \pm 0.47) \times 10^{-6}$	$(6.93 \pm 0.59) \times 10^{-12}$	−21.1
G23NrA	$(2.68 \pm 0.42) \times 10^{-6}$	$(4.31 \pm 0.47) \times 10^{-12}$	−21.5
G23Ch	$(1.47 \pm 0.33) \times 10^{-5}$	$(8.48 \pm 2.77) \times 10^{-10}$	−17.6

[a] Determined by the surface plasmon resonance technique as described in Materials and Methods. [b] Determined by electrophoretic mobility shift titrations as described in Materials and Methods. [c] Calculated for a temperature of 277 K. All values reported represent the mean of at least three determinations ± SEM.

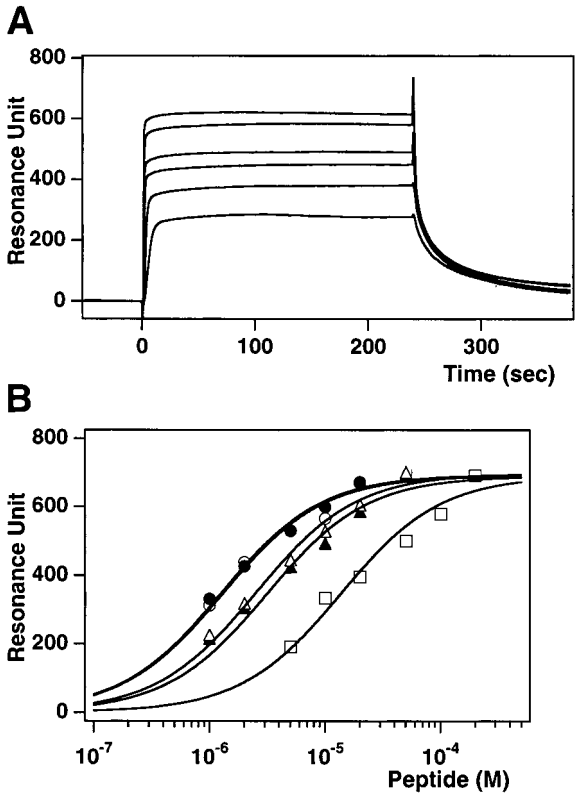

FIGURE 2: (A) Sensorgram showing the interactions between G23Ad and G23Cd at various concentrations. Data from serial injections of G23Ad at concentrations from 1, 2, 5, 10, 20, and 50 μM (from bottom to top) over the surface with G23Cd immobilized are shown. (B) Comparison of the binding of G23Ad, G23NAd, G23NrA, G23Nb, and G23Ch to G23Cd. The response at equilibrium was plotted vs the concentration for G23Ad/G23Cd (○), G23NAd/G23Cd (●), G23NrA/G23Cd (△), G23Nb/G23Cd (▲), and G23Ch/G23Cd (□). The curves represent the titration binding isotherms calculated from eq 1 using the mean dissociation constants obtained from individual experiments.

Reactions of binding of G23Ad, G23NAd, G23NrA, G23Nb, and G23Ch to G23Cd were monitored at various concentrations of the G23-guest peptides at 10 °C (Figure 2A). Because equilibrium was reached for all these interactions, the equilibrium dissociation constant could be determined by injecting a range of concentrations and plotting the response at equilibrium versus the concentration of injected peptide (Figure 2B). Two different levels of immobilized Cd-peptide were used to avoid the effect of mass transport limitations. The results of these experiments for the G23-guest peptides are summarized in Table 1. The equilibrium dissociation constant (K_{d1}) for the G23Ad/G23Cd dimer was smaller than that reported for the complex of β-cyclodextrin and adamantaneacetic acid (*30*). The G23NAd/G23Cd complex was almost as stable as G23Ad/G23Cd, while G23Nb/G23Cd and G23NrA/G23Cd were only half as stable. The stability of G23Ch/G23Cd was 1 order of magnitude lower than that of G23Ad/G23Cd.

DNA Binding of G23-Guest/G23Cd Dimers to the Native GCN4 Binding Sequence. To explore whether the stability of host−guest complexes affects the cooperative formation of peptide dimer−DNA complexes, we have compared the binding of the G23-guest/G23Cd heterodimers to AP20 by electrophoretic mobility shift titrations (*34*, *35*) in 20 mM Tris-HCl (pH 7.5) containing 4 mM KCl, 2 mM $MgCl_2$, and 1 mM EDTA at 4 °C (Figure 3A). G23Ad/G23Cd, G23NAd/G23Cd, G23NrA/G23Cd, and G23Nb/G23Cd showed almost equal affinities for AP20. In contrast, G23Ch/G23Cd did not form a stable DNA complex efficiently. As judged from the dissociation constant of the G23Ad/G23Cd complex, more than 95% of the G23Ad and G23Cd are free below 100 nM; hence, the reaction of binding of G23Ad and G23Cd to DNA could also be described as a stepwise reaction as proposed for LexA (*38*) and bZIP (*39*, *40*). Because only a mobility-shifted band corresponding to the dimer−DNA complex was observed with the electrophoretic mobility shift assay of the binding reaction mixture containing both the G23-guest and G23Cd peptides, binding equilibria involved in the overall binding reaction were considered as eqs 2 and 3 in this study (see Materials and Methods). Regardless of the pathway used to assemble the dimer−DNA complex, binding of pre-assembled dimers in a single step or two monomers sequentially with dimerization occurring on the DNA, the correct apparent equilibrium dissociation constants could be obtained (*41*) by fitting the data using nonlinear least-squares analysis to eq 17 as described in Materials and Methods (Figure 3B). Using the dissociation constants for G23Cd and the G23-guest peptides (K_{d1}), the equilibrium constants for G23Ad/G23Cd, G23NAd/G23Cd, G23NrA/G23Cd, G23Nb/G23Cd, and G23Ch/G23Cd dimer dissociation with AP20 (K_{d2}) and the overall binding free energy of the dimer−DNA complexes (ΔG) were obtained (Table 1). The dimers with similar K_{d1} values showed almost equal affinities for AP20 with the binding free energy difference being within 0.6 kcal/mol. In contrast, increasing the K_{d1} value by a factor of 10 resulted in the loss of efficient cooperative binding as revealed in the case of G23Ch/G23Cd.

Sequence Selectivity of the G23-Guest/G23Cd Complexes. We next examined whether the guest molecule could modulate the sequence selectivity of dimers. GCN4 has been shown to bind to a nonpalindromic AP1 sequence (5′-ATGACTCAT-3′) and a palindromic CRE sequence (5′-ATGACGTCAT-3′) with roughly equal affinity despite the difference in the spacing between the two half-sites (*41*−*43*). Because a number of studies have been carried out to evaluate the sequence selective binding of GCN4 and its derivatives using these sequences with different half-site spacing (*23*, *41*−*43*), the affinities of G23-guest/G23Cd dimers for AP20 were compared with those for CRE21 and CGG22. CRE21 contained the palindromic CRE sequence, whereas CGG22 contained a nonpalindromic 5′-ATGACG-GTCAT-3′ sequence. The affinity of G23Ad/G23Cd and G23Nb/G23Cd, which had K_{d1} values of 1.34×10^{-6} and

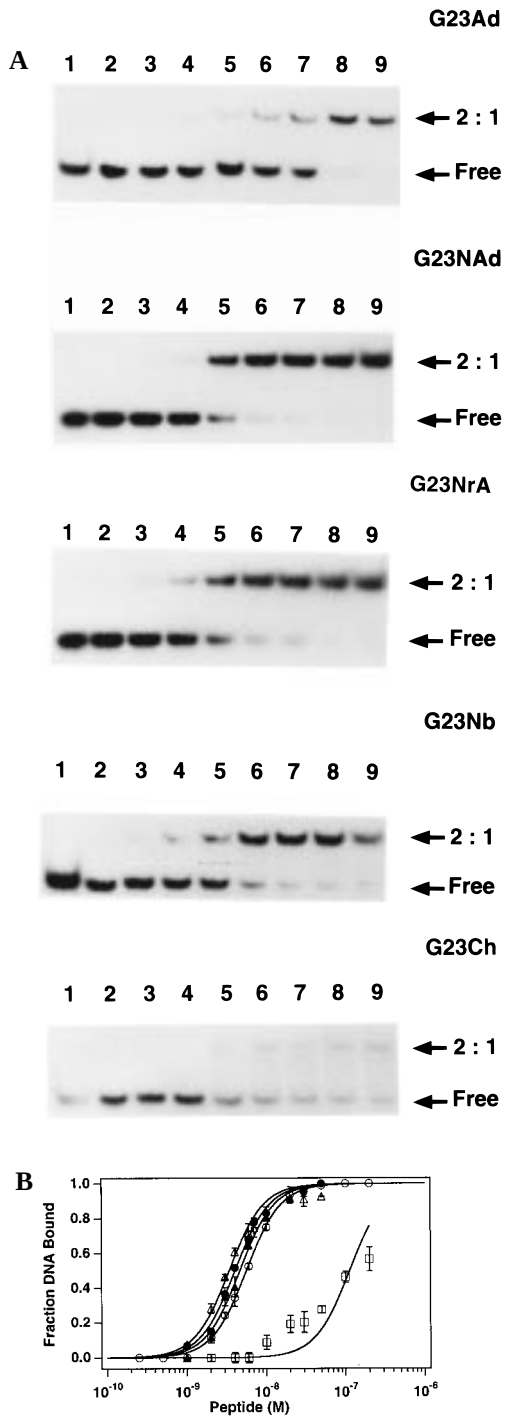

FIGURE 3: (A) Autoradiograms showing the electrophoretic mobility shift titrations (*34*, *35*) of G23-guest/G23Cd heterodimers with AP20 in 20 mM Tris-HCl (pH 7.5) containing 4 mM KCl, 2 mM $MgCl_2$, and 1 mM EDTA at 4 °C. The guest peptide used in each experiment is indicated at right above of each autoradiogram. Arrows denote the free DNA and the dimer−DNA complex. Peptide concentrations in lanes 2−9 were 0.5, 1, 2, 3, 4, 6, 10, and 20 nM for G23Ad, 1, 2, 3, 5, 7, 10, 50, and 100 nM for G23NAd and G23NrA, 1, 2, 3, 4, 6, 10, 20, and 30 nM for G23Nb, and 2, 4, 6, 10, 20, 30, 50, and 100 nM for G23Ch, respectively. (B) Semilogarithmic plots show the fraction of ^{32}P-labeled AP20 DNA bound to G23Ad/G23Cd (○), G23NAd/G23Cd (●), G23NrA/G23Cd (△), G23Nb/G23Cd (▲), and G23Ch/G23Cd (□) as a function of peptide concentration. The data points represent the average of three experiments. The sigmoidal curves represent the titration binding isotherms calculated from eq 17 using the mean dissociation constants obtained from individual experiments.

3.09×10^{-6} M, respectively, for CRE21 and CGG22 were determined by electrophoretic mobility shift titrations (Figure 4A). These data were fitted using nonlinear least-squares analysis to eq 17 as described above (Figure 4B). Using the dissociation constant (K_{d1}) obtained as described above, equilibrium constants for dimer dissociation with CRE21 and CGG22 (K_{d2}) and the overall binding free energy of the dimer−DNA complexes were obtained for the G23Ad/G23Cd and G23Nb/G23Cd dimers (Table 2).

The G23Ad/G23Cd−CRE21 complex was 1.3 and 1.8 kcal/mol more stable than the corresponding AP1 and CGG complexes, respectively, at 4 °C. Changing the adamantyl group into the norbornyl group did not alter the preferential binding of the dimer to CRE21 over AP20 and CGG22. G23Ad/G23Cd and G23Nb/G23Cd showed almost the same affinities for CRE21. However, G23Ad/G23Cd exhibited a slightly higher selectivity (0.5 kcal/mol) for AP20 over CGG22 than did G23Nb/G23Cd.

Correlation between the Helical Content of the Basic Region Peptide and the Stability of Its DNA Complex. The results shown above indicated that the G23Ad/G23Cd dimer preferentially bound to CRE21 over AP20 and CGG22. However, it was unlikely that the direct interaction between the Ad/Cd dimerization domain and the target DNA sequence determined the observed selectivity for the half-site spacing. We considered the possibility that the Ad/Cd dimerization domain determined the selectivity of the half-site spacing by exerting its effect on the proximal region of the basic region peptide as suggested by Schepartz and co-workers for the basic region dimer with a transition metal complex (*23*). The basic region of GCN4 has disordered structure in the complex with a nonspecific DNA, but is structured to an α-helix upon binding to a specific DNA sequence (*17*, *18*, *28*, *44*−*49*). Thus, a subtle difference in the helical structures might be detected in the DNA binding complexes of G23Ad/G23Cd with specific and nonspecific DNA sequences.

Structures of the peptide in the G23Ad/G23Cd complex were analyzed by circular dichroism (CD) spectroscopy in the presence of CRE21, AP20, CGG22, and a nonspecific DNA sequence, NON (Figure 5). The CD signal at 222 nm, a measure of α-helicity, was increased significantly on addition of CRE21 to G23Ad/G23Cd. The difference CD spectrum indicated that the G23 peptide in G23Ad/G23Cd became almost 100% helical upon binding to CRE21, as observed for native GCN4 (*28*, *44*−*49*) and GCN4 basic region peptide dimers (*11*, *17*, *18*, *21*, *25*). With AP20 and CGG22, the helical contents of G23 in the dimer−DNA complexes decreased in the order CRE21 > AP20 > CGG22, which was parallel to the decreasing order of stability for these dimer−DNA complexes. The difference in the helical contents between CGG22 and AP20 was much larger than that between AP20 and CRE21. No obvious change in the intensity of the CD signal at 222 nm was observed on addition of the nonspecific oligonucleotide, NON.

DISCUSSION

Effect of the Host−Guest Interaction on the Overall Stability of the Peptide Dimer−DNA Complexes. In this study, we have explored the sequence-specific DNA binding of the basic region peptide dimers with a variety of dimerization abilities. The dissociation constants for the

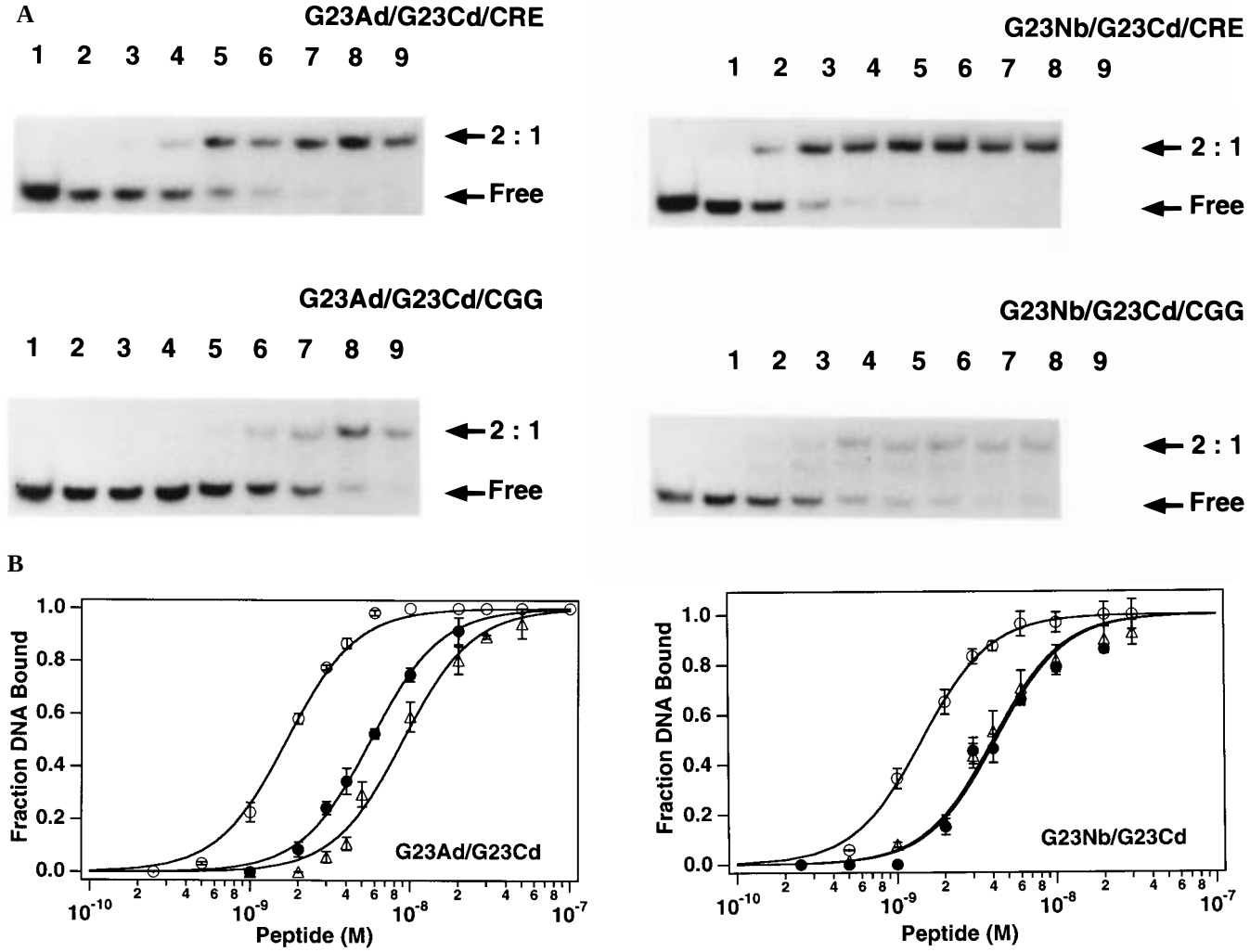

FIGURE 4: (A) Autoradiograms showing the electrophoretic mobility shift titrations (*34*, *35*) of G23Ad/G23Cd (left) and G23Nb/G23Cd (right) heterodimers with CRE21 (upper) and CGG22 (lower) in 20 mM Tris-HCl (pH 7.5) containing 4 mM KCl, 2 mM $MgCl_2$, and 1 mM EDTA at 4 °C. Arrows denote the free DNA and the dimer−DNA complex. Peptide concentrations in lanes 2−9 were 0.5, 1, 2, 3, 4, 6, 10, and 20 nM, respectively. (B) Semilogarithmic plots show the fraction of ^{32}P-labeled CRE21 (○), AP20 (●), and CGG22 (△) bound to G23Ad/G23Cd (left) and G23Nb/G23Cd (right) as a function of peptide concentrations. The data points represent the average of three experiments. The sigmoidal curves represent the titration binding isotherms calculated from eq 17 using the mean dissociation constants obtained from individual experiments.

Table 2: Equilibrium Dissociation Constants K_{d2} and the Binding Free Energy for the G23Ad/G23Cd and G23Nb/G23Cd Complexes with CRE21 and CGG22

	K_{d2} (M)[a]	ΔG (kcal/mol)[b]
G23Ad/G23Cd−CRE21	$(2.13 \pm 0.15) \times 10^{-12}$	−22.2
G23Ad/G23Cd−CGG22	$(5.97 \pm 0.65) \times 10^{-11}$	−20.4
G23Nb/G23Cd−CRE21	$(6.68 \pm 0.39) \times 10^{-13}$	−22.4
G23Nb/G23Cd−CGG22	$(4.76 \pm 0.46) \times 10^{-12}$	−21.3

[a] Determined by electrophoretic mobility shift titrations as described in Materials and Methods. [b] Calculated for a temperature of 277 K. All values reported represent the mean of at least three determinations ± SEM.

G23Ad/G23Cd, G23NAd/G23Cd, G23NrA/G23Cd, and G23Nb/G23Cd dimers (K_{d1}) ranged from 1.32×10^{-6} to 3.09×10^{-6} M. These dimers bound to AP20 with the binding free energy difference being within 0.6 kcal/mol, which was similar to the free energy difference in the stability of these dimers (0.5 kcal/mol). Increasing the K_{d1} value by a factor of 10 (1.47×10^{-5} M) resulted in the loss of efficient cooperative binding as observed for G23Ch/G23Cd. Thus, the stability of the heterodimer−DNA complex appeared to

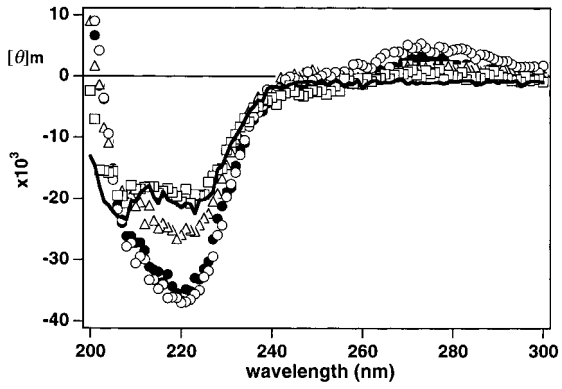

FIGURE 5: Circular dichroism difference spectra for G23Ad/G23Cd in the absence or presence of various DNA indicate that G23Ad/G23Cd is helical when bound to the CRE21, AP20, or CGG22 DNA. Spectra in the absence of DNA (—) and in the presence of CRE21 (○), AP20 (●), CGG22 (△), and NON (□). Spectra of the peptides in the presence of oligonucleotides were calculated as the difference between the bound spectrum and a spectrum of the respective free oligonucleotide (*11*, *25*). CD spectra were obtained as described in Materials and Methods.

be controlled by the stability of the heterodimer. However, there is no linear correlation between the stability of the inclusion complex and that of the dimer−DNA complex in the cases of peptides with the adamantyl, norbornyl, and noradamantyl groups. In addition, the loss of efficient cooperative binding for G23Ch/G23Cd indicated that a minimal energetic requirement existed for the stability of the dimerization domain to cooperatively form the dimer complex at the specific DNA sequence. The lack of efficient cooperative binding of dimer to the specific DNA sequence was observed when the free energy gain in the formation of the host−guest complex was <6.1 kcal/mol, while the efficiency of cooperative dimer formation remained similar when the free energy gain was higher than that.

Interestingly, G23 peptides modified with *N*-(iodoacetyl)-2-aminonaphthalene-6-sulfonate and G23Cd did not form a heterodimer complex with AP20 (data not shown), even though *N*-(iodoacetyl)-2-aminonaphthalene-6-sulfonate and β-cyclodextrin were reported to form an inclusion complex with a stability comparable to that with adamantaneacetic acid (*30*). The ball-like shape of Ad, NAd, NrA, or Nb appeared to be favored for efficient formation of a stable inclusion complex in the specific dimer−DNA complex. Thus, the shape of the guest molecule, in addition to the stability of the inclusion complex, also affected the cooperative formation of the dimer−DNA complex.

Sequence Selectivity of the G23-Guest/G23Cd Complex. Native GCN4 preferentially binds the nonpalindromic AP1 sequence over the palindromic CRE sequence. Discrimination of the half-site spacing by the G23Ad/G23Cd complex was confirmed by gel mobility shift titration experiments with CRE21, AP20, and CGG22. The G23Ad/G23Cd dimer preferentially bound CRE21 over AP20 and CGG22 (Tables 1 and 2). Under the same conditions, a covalently bonded G23 dimer with the 9,10-dihydroxy-9,10-dihydrophenanthrene dimerization domain (*25*) bound to AP20, CRE21, and CGG22 with dissociation constants of 3.5×10^{-10}, 2.5×10^{-10}, and 4.0×10^{-10} M, respectively. Disulfide dimers of the GCN4 basic region with the Gly-Gly-Cys linker bound to CRE and AP1 sites with comparable affinities (*17*, *18*, *21*−*23*), but a covalently bonded basic region dimer with a transition metal complex revealed a remarkable level of specificity (3.3 kcal/mol) for the CRE over the AP1 site (*21*−*23*). Thus, the noncovalent nature of the G23Ad/G23Cd dimerization domain is not the essential determinant for the preferential binding of G23Ad/G23Cd to the CRE sequence. Dimerization domains of the above-mentioned GCN4 basic region peptide dimers were different from each other in the geometry, flexibility, and spacing between two peptides. The inclusion complex of β-cyclodextrin and a guest molecule was much larger than the Gly-Gly-Cys linker or the 9,10-dihydroxy-9,10-dihydrophenanthrene dimerization domain. Because the peptide dimers with bulky dimerization domains such as a transition metal complex and β-Cd/Ad showed preferential binding to the CRE sequence over AP1, a steric factor of the dimerization domain seemed to play critical roles in discriminating the half-site spacing by the basic region peptide dimers. In fact, even a subtle difference in the shape of the dimerization domain affected the stability of the dimer−DNA complex, as obviously shown in the cases of G23Nb/G23Cd and G23Ad/G23Cd.

The Ad/Cd dimerization domain seemed to determine the selectivity of the half-site spacing by exerting its effect on the proximal region of the basic region peptide. As judged from the stabilities of G23Ad/G23Cd−CRE21, −AP20, and −CGG22 complexes (Tables 1 and 2), more than 95% of the G23Ad/G23Cd dimer should form DNA complexes with the target sequences at the peptide concentrations of 4 μM used for the CD measurements. It is therefore unlikely that the presence of free Ad and Cd peptides caused the observed difference in the helical contents of G23Ad/G23Cd−CRE21, −AP20, and −CGG22 complexes. Because the basic region of bZIP forms an α-helical structure only in the presence of specific DNA sequence, the difference in the helical contents for these dimers most likely resulted from a difference in the helical structure of these G23Ad/G23Cd−DNA complexes. The G23 peptides in the dimer−DNA complex would deform the structure at the C-terminus so as to obtain the maximal interactions (1) from the specific interactions between amino acid residues and the DNA surface of two half-sites and (2) from the host−guest inclusion complex. With increasing separation between the two half-sites, as in the case of CGG22, the structural deformation of G23 would extend to a much larger region as compared to the case of CRE21. Such an effect would decrease the stability of the dimer−DNA complex that in turn resulted in the observed sequence selectivity of G23Ad/G23Cd. Whether the dimerization employs a covalent or a noncovalent linkage, the dimerization domain itself would dictate the sequence selectivity of the dimer without directly contacting DNA.

It should be noted that the helical content of G23 in the presence of NON did not increase significantly in this study and other studies in which the basic region peptides were used (*11*−*13*, *17*, *18*, *21*, *25*, *26*, *44*, *46*). A recent model study in which short peptides containing Ala and Lys residues were used suggested that helical conformation of the basic region may be generally present in nonspecific as well as specific complexes between bZIP transcription factors and DNA (*50*). Contrary to the case of Ala-Lys peptides, the helical content of basic region peptide G23 increased with increasing stability of the G23Ad/G23Cd dimer−DNA complex. The induced fit mechanism (*51*) takes place at least in the sequence-specific DNA binding of the basic region peptide.

Origin of the Cooperative Interaction Energy. An interaction energy responsible for the cooperative formation of these dimer−DNA complexes could be estimated by using the overall stabilities of the dimer−DNA complexes and that of the complex between the 5′-ATGAC-3′ half-site (HS) and G23Ad ($\Delta G = -9.2 \pm 0.2$ kcal/mol at 4 °C) (*13*). The cooperative interaction energy for the formation of the dimer−AP20 complexes (ΔG_{coop}) was expressed as $\Delta G_{coop} = \Delta G_{(G23-guest/G23Cd-DNA)} - \Delta G_{(G23-guest-HS)} - \Delta G_{(G23Cd-HS)}$. By assuming that the G23-guest peptides and G23Cd bound the 5′-ATGAC-3′ half-site with the same affinities, the ΔG_{coop} values for the dimer−AP20 complexes were estimated as summarized in Table 3. The cooperative interaction energy values of 2.5−3.1 kcal/mol obtained in our system are comparable to those of cooperative binding repressor proteins (*2*, *52*) and oligonucleotides in triple helix formation (*53*−*58*). Even higher cooperative interaction energies were obtained for G23Ad/G23Cd− and G23Nb/G23Cd−CRE21 complexes.

Table 3: Estimated Cooperative Interaction Energies (Kilocalories per Mole) for Dimer−DNA Complexes

	$\Delta G_{host-guest}$[a]	ΔG_{coop}[b]	$\Delta G_{anti-coop}$[c]
G23Ad/G23Cd−AP20	−7.4	−2.5	4.9
G23NAd/G23Cd−AP20	−7.5	−2.9	4.6
G23Nb/G23Cd−AP20	−7.0	−2.7	4.3
G23NrA/G23Cd−AP20	−7.1	−3.1	4.0
G23Ch/G23Cd−AP20	−6.1	0.8	6.9
G23Ad/G23Cd−CRE21	−7.4	−3.8	3.6
G23Ad/G23Cd−CGG22	−7.4	−2.0	5.4
G23Nb/G23Cd−CRE21	−7.0	−4.0	3.0
G23Nb/G23Cd−CGG22	−7.0	−2.9	4.1

[a] Determined by the surface plasmon resonance technique as described in Materials and Methods. [b] Calculated as $\Delta G_{(G23-guest/G23Cd-DNA)} - \Delta G_{(G23Ad-HS)} - \Delta G_{(G23Cd-HS)}$ with $\Delta G_{(G23-guest/G23Cd-DNA)}$ values taken from Tables 1 and 2 and $\Delta G_{(G23Ad-HS)} = \Delta G_{(G23Cd-HS)} = -9.2$ kcal/mol. [c] Calculated as $\Delta G_{coop} - \Delta G_{host-guest}$.

In this study, potential sources for the cooperative interaction energy include host−guest inclusion complex formation ($\Delta G_{host-guest}$) and interactions that act against the cooperative binding ($\Delta G_{anti-coop}$) such as the steric interference on dimer formation. Inspection of the $\Delta G_{anti-coop}$ values in Table 3 indicates that a certain level of binding free energy between β-cyclodextrin and a guest molecule, ~7 kcal/mol in this case, was necessary for the cooperative formation of the specific dimer−DNA complex. The observed decrease in the helical content, which was possibly dictated by the structural deformation of the peptide in the region proximal to the dimerization domain as discussed above, might be related to the free energy acting against the cooperative binding ($\Delta G_{anti-coop}$) in Table 3. Thus, the minimal energetic requirement for the cooperative formation of a dimer-specific DNA complex would be highly correlated with the binding free energy and the structure of the host−guest complex. Another source that would affect the cooperative binding of the peptide dimer is the affinity of the peptide monomer for the target DNA sequence. It will be interesting to compare the cooperative interaction energies for these GCN4 basic region dimers with that for other basic region peptide dimers with the same dimerization domains.

REFERENCES

1. Jones, N. (1990) *Cell 61*, 9−11.
2. Ptashne, M. (1986) *A Genetic Switch*, Blackwell Scientific Publications and Cell Press, Palo Alto, CA.
3. Harrison, S. C., and Aggarwal, A. K. (1990) *Annu. Rev. Biochem. 59*, 933−969.
4. Pabo, C. O., and Sauer, R. T. (1992) *Annu. Rev. Biochem. 61*, 1053−1095.
5. Harrison, S. C. (1991) *Nature 353*, 715−719.
6. Adhya, S. (1989) *Annu. Rev. Genet. 23*, 227−250.
7. Tijan, R., and Maniatis, T. (1994) *Cell 77*, 5−8.
8. Brenowitz, M., Mandal, N., Pickar, A., Jamison, E., and Adhya, S. (1991) *J. Biol. Chem. 266*, 1281−1288.
9. Beckett, D., Burz, D. S., Ackers, G. K., and Sauer, R. T. (1993) *Biochemistry 32*, 9073−9079.
10. Chen, J., and Matthews, K. S. (1994)*Biochemistry 33*, 8728−8735.
11. Ueno, M., Murakami, A., Makino, K., and Morii, T. (1993) *J. Am. Chem. Soc. 115*, 12575−12576.
12. Ueno, M., Sawada, M., Makino, K., and Morii, T. (1994) *J. Am. Chem. Soc. 116*, 11137−11138.
13. Morii, T., Yamane, J., Aizawa, Y., Makino, K., and Sugiura, Y. (1996) *J. Am. Chem. Soc. 118*, 10011−10017.
14. Hurst, H. C. (1994) *Protein Profile 1*, 123−168.
15. Hinnebusch, A. G. (1984) *Proc. Natl. Acad. Sci. U.S.A. 81*, 6442−6446.
16. Landschultz, W. H., Johnson, P. F., Adashi, E. Y., Graves, B. J., and McKnight, S. L. (1988) *Genes Dev. 2*, 786−800.
17. Talanian, R. V., McKnight, C. J., and Kim, P. S. (1990) *Science 249*, 769−771.
18. Talanian, R. V., McKnight, C. J., Rutkowski, R., and Kim, P. S. (1992) *Biochemistry 31*, 6871−6875.
19. Park, C., Campbell, J. L., and Goddard, W. A., III (1992) *Proc. Natl. Acad. Sci. U.S.A. 89*, 9094−9096.
20. Park, C., Campbell, J. L., and Goddard, W. A., III (1995) *J. Am. Chem. Soc. 117*, 6287−6291.
21. Cuenoud, B., and Schepartz, A. (1993) *Science 259*, 510−513.
22. Cuenoud, B., and Schepartz, A. (1993) *Proc. Natl. Acad. Sci. U.S.A. 90*, 1154−1159.
23. Palmer, C. R., Sloan, L. S., Adrian, J. C., Jr., Cuenoud, B., Paolella, D. N., and Schepartz, A. (1995) *J. Am. Chem. Soc. 117*, 8899−8907.
24. Morii, T., Shimomura, M., Morimoto, M., and Saito, I. (1993) *J. Am. Chem. Soc. 115*, 1150−1151.
25. Okagami, M., Ueno, M., Makino, K., Shimomura, M., Saito, I., Morii, T., and Sugiura, Y. (1995) *Bioorg. Med. Chem. 3*, 777−784.
26. Morii, T., Saimei, Y., Okagami, M., Makino, K., and Sugiura, Y. (1997) *J. Am. Chem. Soc. 119*, 3649−3655.
27. Pellegrini, M., and Ebright, R. H. (1996) *J. Am. Chem. Soc. 118*, 5831−5835.
28. Ellenberger, T. E., Brandl, C. J., Struhl, K., and Harrison, S. C. (1992) *Cell 71*, 1223−1237.
29. Smith, T. J. (1995) *J. Mol. Graphics 13*, 122−125.
30. Eftink, M. R., Andy, M. L., Bystrom, K., Perlmutter, H. D., and Kristol, D. S. (1989) *J. Am. Chem. Soc. 111*, 6765−6772.
31. Inoue, Y., Hakushi, T., Liu, Y., Tong, L.-H., Shen, B.-J., and Jin, D.-S. (1993) *J. Am. Chem. Soc. 115*, 475−481.
32. Melton, L. D., and Slessor, K. N. (1971) *Carbohydr. Res. 18*, 29−37.
33. Maniatis, T., Fritsch, E. F., and Sambrook, J. (1987) *Molecular Cloning: A Laboratory Manual*, Cold Spring Harbor Laboratory Press, Cold Spring Harbor, NY.
34. Freid, M., and Crothers, D. M. (1981) *Nucleic Acids Res. 9*, 6505−6525.
35. Gamer, M. M., and Revzin, A. (1981) *Nucleic Acids Res. 9*, 3047−3060.
36. Jönsson, U., Fägerstam, L., Roos, H., Rönnberg, J., Sjölander, S., Stenberg, E., Stahlberg, R., Urbaniczky, C., Östlin, H., and Malmqvist, M. (1991) *BioTechniques 11*, 620−627.
37. Atherton, E., and Sheppard, R. C. (1985) *J. Chem. Soc., Chem. Commun.*, 165−166.
38. Kim, B., and Little, J. W. (1992) *Science 255*, 203−206.
39. Park, C., Campbell, J. L., and Goddard, W. A., III (1996) *J. Am. Chem. Soc. 118*, 4235−4239.
40. Metallo, S. J., and Schepartz, A. (1997) *Nat. Struct. Biol. 4*, 115−117.
41. Metallo, S. J., and Schepartz, A. (1994) *Chem. Biol. 1*, 143−151.
42. Sellers, J. W., Vincent, A. C., and Struhl, K. (1990) *Mol. Cell. Biol. 10*, 5077−5086.
43. Paolella, D. N., Palmer, C. R., and Schepartz, A. (1994) *Science 264*, 1130−1133.
44. Weiss, M. A., Ellenberger, T., Wobble, C. R., Lee, J. P., Harrison, S. C., and Struhl, K. (1990) *Nature 347*, 575−578.
45. Weiss, M. A. (1990) *Biochemistry 29*, 8020−8024.
46. O'Neil, K. T., Shuman, J. D., Ampe, C., and DeGrado, W. F. (1991) *Biochemistry 30*, 9030−9034.
47. Saudek, V., Pasley, H. S., Gibson, T., Gausepohl, H., Frank, R., and Pastore, A. (1991) *Biochemistry 30*, 1310−1317.
48. König, P., and Richmond, T. J. (1993) *J. Mol. Biol. 233*, 139−154.
49. Keller, W., König, P., and Richmond, T. J. (1995) *J. Mol. Biol. 254*, 657−667.
50. Johnson, N. P., Lindstrom, J., Baase, W. A., and von Hippel, P. H. (1994) *Proc. Natl. Acad. Sci. U.S.A. 91*, 4840−4844.
51. Frankel, A. D., and Kim, P. S. (1991) *Cell 65*, 717−719.

52. Ackers, G. K., Johnson, A. D., and Shea, M. A. (1982) *Proc. Natl. Acad. Sci. U.S.A. 79*, 1129−1133.
53. Distefano, M. D., Shin, J. A., and Dervan, P. B. (1991) *J. Am. Chem. Soc. 113*, 5901−5902.
54. Colocci, N., Distefano, M. D., and Dervan, P. B. (1993) *J. Am. Chem. Soc. 115*, 4468−4473.
55. Distefano, M. D., and Dervan, P. B. (1993) *Proc. Natl. Acad. Sci. U.S.A. 90*, 1179−1183.
56. Colocci, N., and Dervan, P. B. (1994) *J. Am. Chem. Soc. 116*, 785−786.
57. Colocci, N., and Dervan, P. B. (1995) *J. Am. Chem. Soc. 117*, 4781−4787.
58. Szewczyk, J. W., Baird, E. E., and Dervan, P. B. (1996) *J. Am. Chem. Soc. 118*, 6778−6779.

BI9828829